Letter | Editors' Suggestion

Driven anti-Bragg subradiant correlations in waveguide quantum electrodynamics

Alexander N. Poddubny *
Ioffe Institute, St. Petersburg 194021, Russia

(Received 27 February 2022; revised 17 August 2022; accepted 8 September 2022; published 29 September 2022)

We study theoretically driven quantum dynamics in periodic arrays of two-level qubits coupled to the waveguide. We demonstrate that strongly subradiant eigenstates of the master equation for the density matrix emerge under strong coherent driving for arrays with the anti-Bragg periods $d = \lambda/4, 3\lambda/4 \ldots$. This happens even though are no such eigenstates at low driving powers and is directly manifested by long-living quantum correlations between the qubits.

DOI: 10.1103/PhysRevA.106.L031702

Introduction. Many-body quantum systems in the presence of driving and dissipation are now a subject of active studies. It is now understood that their dynamics is not limited to conventional relaxation to the ground state and thermalization. Instead, the system can exhibit many-body localization [1,2], or even more exotic time-crystalline phases that break discrete time-translational symmetry under the presence of external driving and oscillate in time instead of decaying to the time-independent stationary phase [3–6]. Here, we predict the formation of driving-induced correlations, immune to radiative dissipation in the waveguide quantum electrodynamics (WQED) platform, shown in Fig. 1, where a periodic array of qubits is coupled to photons in a waveguide [7–11].

The suppression of spontaneous emission by destructive interference has been known at least since the work of Dicke [12]. Briefly, two quantum emitters can be excited with opposite phases to the state $|\psi\rangle = (\sigma_1^\dagger - \sigma_2^\dagger)|0\rangle/\sqrt{2}$ (here, $\sigma_{1,2}^\dagger$ are the raising operators). Subradiant states have been also extensively studied in the last several years for arrays of qubits coupled to the waveguide, both theoretically [13–17] and experimentally [18,19]. Nevertheless, to the best of our knowledge, previously considered subradiant states are very distinct from those studied here. First, typical subradiant states exist only for relatively low filling factors of the array [13]. Specifically, it has been proven in our recent work [20] that many-body subradiant eigenstates of the effective non-Hermitian Hamiltonian of the array disappear for fill factors above $f = 1/2$ which indicated that they can be seen only under relatively weak driving. Indeed, an increase of the driving strength typically results in the growth of the linewidth and the saturation of optical transitions of a two-level system [21]. Second, a typical subradiant state is a feature of an array with the subwavelength period ($d \ll \lambda$) or, more generally, a Bragg period that is close to any integer multiple of $\lambda/2$ [22]. On the other hand, for two qubits with $\lambda/4$ spacing the waveguide-induced coupling has a purely exchange character: Both eigenmodes have the same lifetime as a single qubit and neither super- nor subradiant states exist. This has been experimentally demonstrated in Ref. [10]. It is however precisely this anti-Bragg regime with $d = \lambda/4, 3\lambda/4, \ldots$ that we focus on here. We predict that while conventional subradiant states do not exist for $d = \lambda/4$ for small values of N, subradiant correlations emerge under strong coherent driving through the waveguide mode. Importantly, these correlations manifest themselves only in the full master equation for the density matrix of the driven system. This explains why they have not previously been revealed in the spectrum of effective many-body Hamiltonians analyzed in Refs. [13–15,17]. On the other hand, in the cavity QED, where the master equation is a standard tool [23–25], spacing between the atoms is a less important parameter and the concepts of Bragg and anti-Bragg spacing are not directly applicable.

The qualitative origin of anti-Bragg driven subradiant correlations is illustrated in Fig. 1(b). Our main finding is that strong coherent electromagnetic driving at the qubit resonance frequency effectively splits the array into two parts, including only odd-numbered and only even-numbered qubits, respectively, i.e., the exchange photon-mediated interaction between these two subarrays is suppressed. The driven $\lambda/4$-spaced array behaves akin to two $\lambda/2$-spaced subarrays. In each of the subarrays subradiant states can be understood by analyzing the saturation of transitions between collective spin states [inset in Fig. 1(b)]. Thus, the driving breaks the spatial symmetry of the array and separates a nonsubradiant system into two subradiant ones. Such symmetry breaking is a mesoscopic feature of finite-size arrays that occurs even though the external driving is homogeneous in space, the array is periodic, and has no disorder.

Model. The time dynamics of the density matrix of the system ρ is described by the master equation $\partial_t \rho = \mathcal{L}\rho$, where $\mathcal{L}$ is the Lindblad superoperator [26,27],

$$\mathcal{L}\rho = 2\gamma_{1D} \sum_{m,n=1}^{N} \cos[\varphi(m-n)]\sigma_m \rho \sigma_n^\dagger - i(H^\dagger \rho - \rho H). \tag{1}$$

Here, γ_{1D} is the spontaneous decay rate of a single qubit into the waveguide mode, ω_0 is the qubit resonance frequency,

*poddubny@coherent.ioffe.ru

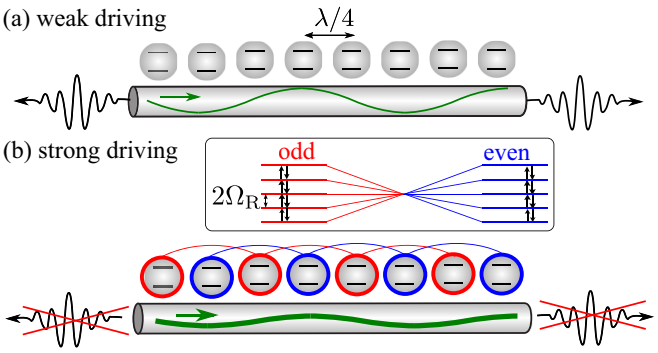

FIG. 1. Schematic illustration of an array of qubits coupled to a waveguide with an anti-Bragg period of $\lambda/4$. (a) and (b) correspond to weak and strong coherent driving from the left-hand side, respectively, illustrated by a green wave. There are no subradiant states for weak driving, while strong driving splits the array into two $\lambda/2$-spaced subarrays with subradiant correlations in each half. The inset illustrates collective spin states after the splitting.

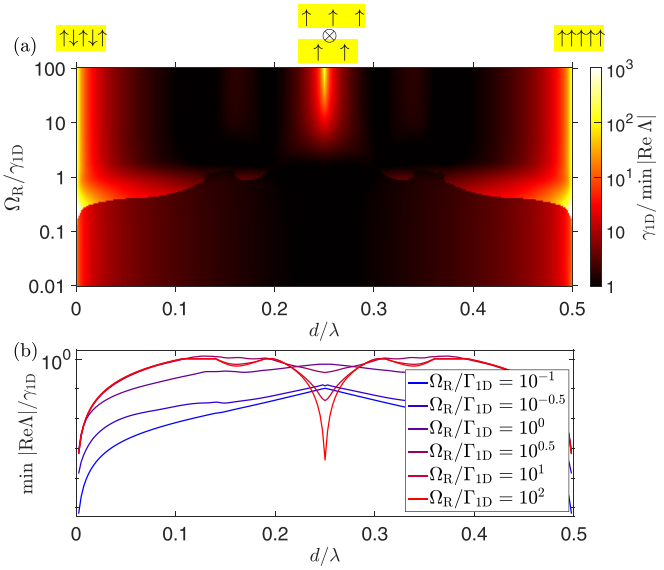

FIG. 2. Dependence of the lifetime of the longest-living correlation on the array period d and the Rabi frequency Ω_R. (a) shows the color map, and (b) shows the cross sections of the color map for several Rabi frequency values indicated on the graph. The symbols on the top of (a) schematically indicate the spin phases. Calculated for $N = 5$.

c is the light speed in the waveguide, and $\varphi \equiv 2\pi d/\lambda$ is the light phase gained between two neighboring qubits. The Hamiltonian reads

$$H = H_0 + V, \quad H_0 = -i\gamma_{1D} \sum_{m,n=1}^{N} \sigma_m^\dagger \sigma_n e^{i\varphi|m-n|}, \qquad (2)$$

where the H_0 term describes the waveguide-induced coupling between the qubits. The non-Hermitian part of H_0 accounts for the spontaneous decay into the waveguide. This Hamiltonian also assumes the usual Markovian and rotating-wave approximations. The interaction term $V = \Omega_R \sum_{n=1}^{N} (\sigma_n^\dagger e^{-i\varphi n} + \text{H.c.})$ is responsible for the resonant coherent driving at the qubit resonance frequency. For simplicity we count all the frequencies from the qubit resonant frequency ω_0.

Many-body time dynamics. In order to provide insight into the time dynamics we study the eigenstates of the master equation defined as $\mathcal{L}\rho = \Lambda\rho$. One of the eigenvalues Λ is always exactly equal to zero, and corresponds to the stationary solution. The real part of the nonzero eigenvalues $-\text{Re}\,\Lambda$ is the spontaneous decay rate of the transient correlations in the presence of the driving. More details are given in the Supplemental Material (SM) [28]. We show in Fig. 2 the dependence of the smallest nonzero rate $-\text{Re}\,\Lambda$ on the Rabi frequency Ω_R and the array period d. Figure 2(a) shows the decay rate as a color map, while Fig. 2(b) presents the map cross sections for specific values of Ω_R. The calculation demonstrates that at low powers, $\Omega_R \ll \gamma_{1D}$, the strongly subradiant correlations exist for d close to 0 and d close to $\lambda(\omega_0)$. They become less subradiant at larger powers [compare the first three curves in Fig. 2(b) calculated for $\Omega_R/\gamma_{1D} = 10^{[-1,0.5,0]}$].

These results at low powers are in full agreement with Refs. [13,14,17,20,33]. However, these previous works, including ours [14,20], have been focused on the eigenstates of the non-Hermitian Hamiltonian H_0 in Eq. (2), that are characterized by a certain integer number of polaritons $\hat{n} = \sum_m \sigma_m^\dagger \sigma_m$. On the other hand, here we consider the master equation in the presence of driving. Hence, the current study captures additional physics at larger powers, $\Omega_R \gg \gamma_{1D}$, that is beyond the effective Hamiltonian approach.

Specifically, it can be seen in Fig. 2 that while strongly subradiant correlations are not present for an anti-Bragg period $d \approx \lambda(\omega_0)/4$ under weak driving, they emerge for $\Omega_R \gg \gamma_{1D}$. This is also manifested as a sharp dip in the middle of the last two red curves in Fig. 2(b). The larger the driving, the longer is the lifetime. An observation of these anti-Bragg subradiant correlations constitutes our main finding.

In order to examine subradiant correlations in more detail we show in Fig. 3 the dependence of the decay rates on Ω_R for $d = \lambda/4$. At low powers, $\Omega_R \ll \gamma_{1D}$, there are no strongly subradiant correlations. The smallest decay rate for $d = \lambda/4$ ($\varphi = \pi/2$) and $N \gg 1$ is given by $\text{Re}\,\Lambda = -\pi^2\gamma_{1D}/N^3$, in contrast to the much smaller decay rate $\text{Re}\,\Lambda \sim \varphi^2\gamma_{1D}/N^3$ in the subwavelength structures where $\varphi \ll \pi$ [13,18,28]. At larger powers, $\Omega_R \lesssim \gamma_{1D}$, these decay rates first increase because qubit transitions are saturated by the driving. However, the spectrum drastically changes for $\Omega_R \gtrsim 10\gamma_{1D}$. Nine eigenvalues split from the rest of the spectrum, and acquire small real parts $\sim\gamma_{1D}^3/\Omega_R^2$ that decrease at larger powers. These are considered anti-Bragg subradiant correlations. Their spatial structure is further examined in Figs. 3(b)–3(d) where we present the correlation function $\text{Tr}[\rho\sigma_n^\dagger\sigma_m]$ for the longest-living correlation at three different powers. With the increase of the driving the correlations acquire a characteristic checkerboard pattern, namely, they exist only for qubit numbers of the same parity. This suggests that the subarrays with odd- and even-numbered qubits, that have $\lambda/2$ spacing [see also Fig. 1(b)], should be analyzed separately at larger powers. The same checkerboard structure exists also in the spin-spin correlation functions calculated for the ground state [28]. The

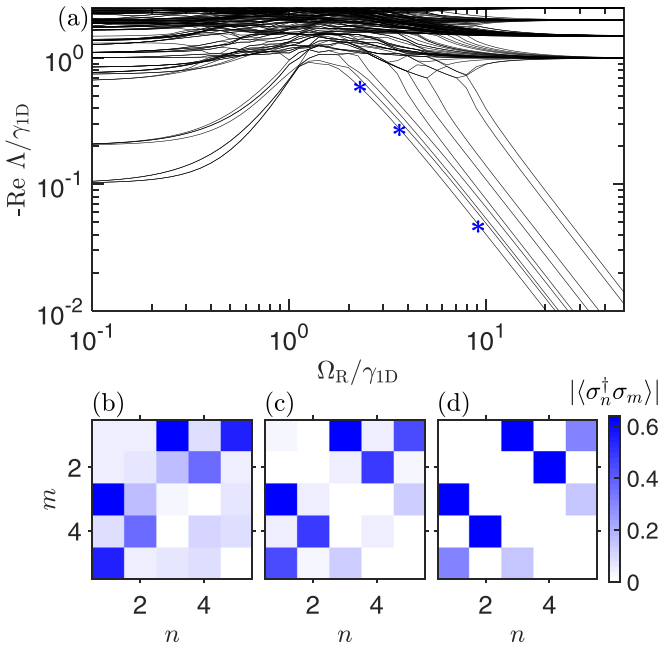

FIG. 3. (a) Dependence of the normalized decay rates on Ω_R for $d = \lambda/4$ and $N = 5$. (b)–(d) Spin-spin correlation function $|\langle\sigma_n^\dagger\sigma_m\rangle|$ calculated for the second longest-living eigenstate for $\Omega_R/\gamma_{1D} = 10^{0.4}, 10^{0.6}, 10^{1}$. These values are also indicated by blue stars in (a).

patterns in Figs. 3(b)–3(d) are mirror asymmetric because the driving is performed from the left of the array.

Eigenstates of effective Hamiltonian. Our approach, focused on the eigenstates of the Lindblad operator (1), might seem redundant since it could be sufficient to consider just the eigenstates of the effective non-Hermitian Hamiltonian H in Eq. (2) that already includes both spontaneous decay into the waveguide and the driving term V. The decay rates are then found as imaginary parts of the Hamiltonian eigenvalues ω and are shown in Fig. 4. Surprisingly, there are no subradiant eigenstates in Fig. 4 at large driving powers, in stark contrast to the more rigorous approach in Fig. 3 that shows the presence of subradiant correlations for $\Omega_R \gg \gamma_{1D}$. Thus, the effective Hamiltonian does not capture the formation of subradiant correlations. This can be qualitatively explained by the underlying assumption that after spontaneous photon emission the quantum state of the qubit array is lost in the effective treatment, while in fact it just decays into the less-excited subspace of the Hilbert space. Thus, the effective Hamiltonian does not fully capture the driven-dissipative dynamics. In other words, the formation of subradiant correlations requires a delicate balance between the spontaneous decay (quantum jump terms in the master equation) and the driving. Unless both these terms are rigorously taken into account, subradiant correlations cannot be adequately described.

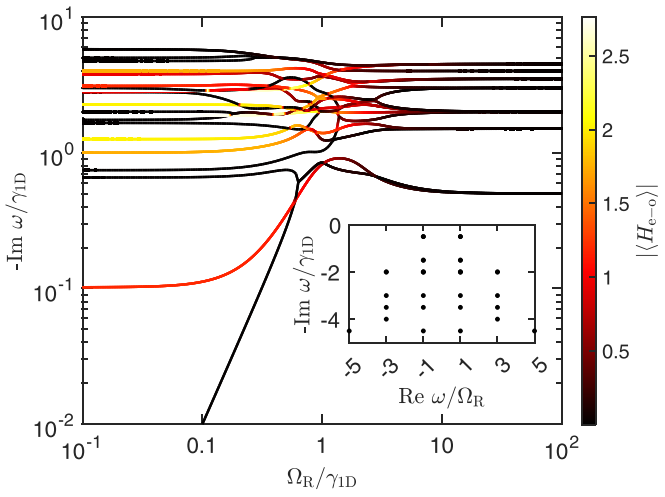

FIG. 4. Decay rates of the eigenstates of the effective Hamiltonian H, Eq. (2). Calculation has been performed for $d = \lambda/4$ and $N = 5$. Color shows the expectation value of the Hamiltonian Eq. (6). The inset shows the complex energy spectrum for $\Omega_R = 100\gamma_{1D}$.

Explanation of subradiant correlations. We start with an auxiliary simplified case of a vanishing array period d, so that $\varphi = 0$. Only the collective spin raising operator, corresponding to the usual Dicke state, $\sigma_{tot} = \sum_{n=1}^{N} \sigma_n$, is then coupled to photons. In particular, the driving term is proportional just to $V = \Omega_R(\sigma_{tot}^\dagger + \sigma_{tot}) \equiv \Omega_R\sigma_{tot,x}$, and the dissipation is governed by the Lindblad operator

$$\mathcal{L}_{diss}\rho = \gamma_{1D}(2\sigma_{tot}\rho\sigma_{tot}^\dagger - \sigma_{tot}^\dagger\sigma_{tot}\rho - \rho\sigma_{tot}^\dagger\sigma_{tot}). \quad (3)$$

It is then convenient to use the basis of the eigenstates $\psi_{J,M}^{(\nu)}$ with the given total collective spin J and its projection $M = -J, -J+1 \ldots J$ onto the x axis. Such collective spin formalism is widely used also in the cavity QED (see, e.g., Refs. [23,25]). Here, the index $\nu = 1 \ldots \chi_J$ distinguishes between different irreducible representations with the same J. For example, for $N = 2$ spins we get the usual triplet ($J = 1$) and a singlet ($J = 0$). For $N = 3$ there exists one quadruplet with $J = 3/2$, and $\chi_{1/2} = 2$ doublets with $J = 1/2$. Subradiant eigenstates can be then sought in a quasidiagonal form

$$\rho^{(\nu,\nu')} = \sum_{M=-J}^{J} |\psi_{J,M}^{(\nu)}\rangle f_M \langle\psi_{J,M}^{(\nu')}|. \quad (4)$$

Since the matrices Eq. (4) are by construction quasidiagonal in the $\psi_{J,M}$ basis, they commute with the driving term, $[V, \rho^{(\nu,\nu')}] = 0$. Next, the master equation $d\rho/dt = \mathcal{L}\rho$ for the matrices Eq. (4) reduces to an effective kinetic Boltzmann equation for the occupation numbers f_M. Namely, we obtain

$$\frac{df_M}{dt} = \gamma_{1D}[W_{M+1}(f_{M+1} - f_M) + W_M(f_{M-1} - f_M)], \quad (5)$$

where $W_M = (J+M)(J-M+1)/2 \equiv \sigma_{tot,M-1,M}^2/2$ [34] (the first and second terms on the right-hand side should be omitted for $M = J$ and $M = -J$, respectively). Equation (5) has a uniform stationary solution $f_M = 1/(2J+1)$ that corresponds to a subradiant correlation, $\mathcal{L}\rho^{(\nu,\nu')} = 0$. Such a uniform solution is especially transparent for just the $N = 1$ qubit, when $J = 1/2$. Then it reduces to a usual saturated state of a strongly driven two-level system, where the ground and excited states have equal populations of $1/2$. Due to the degeneracy in ν, ν', the number of independent subradiant correlations $\rho^{(\nu,\nu')}$ is given by $\sum_J \chi_J^2$, that is, 1,2,5,14 for $N = 1, 2, 3, 4$, respectively. These operators (4) correspond to long-living correlations in Fig. 2 for $\varphi = 0$. Exactly the same analysis is applicable also to the Bragg

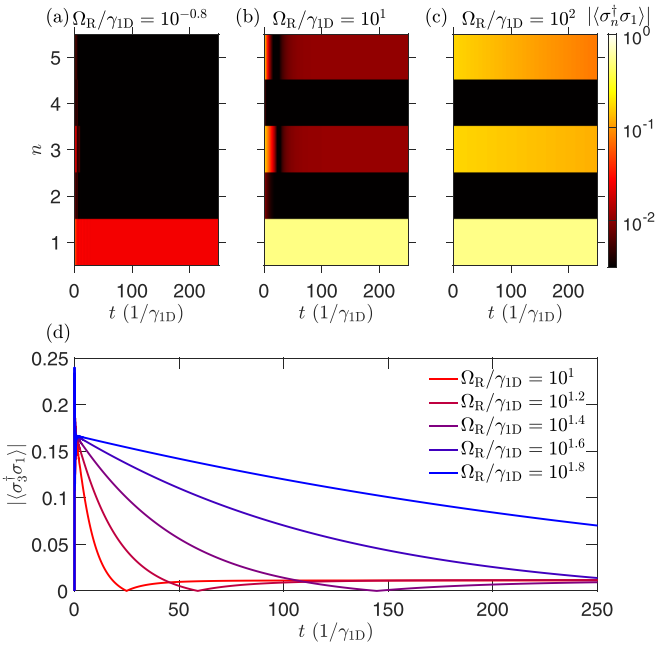

FIG. 5. Time dynamics of the correlation function $\langle\sigma_n^\dagger\sigma_1\rangle$ depending on the driving power. (a)–(c) Dependence of the correlation functions for three different driving strengths, indicated on the graphs. (d) Time dependence of the correlation function $\langle\sigma_3^\dagger\sigma_1\rangle$. Calculation has been performed for $d = \lambda/4$, $N = 5$. At the moment $t = 0$ the array is in the fully excited state.

structures with $d = q\lambda/2$ ($\varphi = q\pi$, $q = 1, 2, \ldots$). The only difference is that the total spin raising operator is given by $\sigma_{\rm tot} = \sum_{n=1}^{N}(-1)^{qn}\sigma_n$.

Subradiant correlations for $\varphi = 0$ and $\varphi = \pi$ are not especially surprising since subradiant eigenstates also exist without driving. Somewhat similar phases have recently been also reported for the related case of cavity QED [25] with incoherent driving. However, we are now in a position to explain also the less expected strongly subradiant correlations for the anti-Bragg case of $\varphi = \pi/2$. The main idea is that the even and odd sublattices of the $d = \lambda/4$-spaced lattice, with $d = \lambda$ spacing, become independent for a strong driving. For a weak driving there exists an exchange coupling between these two sublattices, described by the Hamiltonian

$$H_{\rm e-o} = -i\gamma_{1D}\sum_{k,l}\sigma_{2k}^\dagger\sigma_{2l-1}e^{i\varphi|2k-2k+1|}. \qquad (6)$$

However, such coupling is suppressed when the sublattices are effectively detuned from each other by strong driving. Indeed, the color of the lines in Fig. 4 encodes the expectation values of the Hamiltonian Eq. (6). At large driving the lines become darker, which indicates the quenching of the coupling. This supports our interpretation of Figs. 3(b)–3(d): Two sublattices become independent for $\Omega_R \gg \gamma_{1D}$. As such, subradiant eigenstates of the Lindblad operator for $\varphi = \pi/2$ are products of the corresponding eigenstates (4) for odd- and even-numbered subarrays, $\rho_{\varphi=\pi/2} = \rho^{\rm odd}_{\varphi=\pi} \otimes \rho^{\rm even}_{\varphi=\pi}$. Such an eigenstate factorization is a rather special feature of the $\lambda/4$ spacing. It becomes possible only because the odd-even mixing Hamiltonian Eq. (6) is Hermitian and it is suppressed by the driving, while the dissipative part of the Lindblad operator does not mix the two sublattices, $\cos[\varphi(m-n)] = 0$ for $\varphi = \pi/2$ and odd $m - n$. A more detailed analysis reveals that spontaneous decay is still possible in the Re $\Lambda \sim \gamma_{1D}^3/\Omega_R^2$ order. The perturbation theory to calculate the decay rate is described in Sec. S1B of SM [28]. In particular, for $N = 3$ qubits the rate for the longest-living correlation is approximately given by $59\gamma_{1D}^3/(9\Omega_R^2)$. We also note that there also exist two superradiant correlations, arising at $d = \lambda/4$ for strong driving (see SM [28]), which is consistent without our interpretation of an array split into two.

Potential observation. The considered subradiant eigenstates could be directly observed in the time-dependent correlations between the qubit excitations. The results are shown in Fig. 5 for different driving strengths. We start with the array being fully excited at the moment $t = 0$ and then study the evolution of the correlations $\langle\sigma_n^\dagger\sigma_1\rangle$ depending on the driving strength. For low strength [Fig. 5(a) and red curves in Fig. 5(d)], the correlations for $n > 1$ quickly decay with time. A stronger driving strength leads to the appearance of the significant correlations $\langle\sigma_3^\dagger\sigma_1\rangle$ and $\langle\sigma_5^\dagger\sigma_1\rangle$ at large times. The blue curves in Fig. 5(d) clearly indicate the slowdown of the decay. This is fully consistent with the correlations shown in Fig. 3. A potential experiment would require a superconducting processor with just $N = 3$ anti-Bragg-spaced qubits, which is well within the current technological limits of circuit QED [35].

Outlook. Our findings uncover yet another mechanism of the formation of subradiant correlations in the Dicke-like models. Since the considered subradiant eigenstates have large degeneracy, they should be quite sensitive to the modification of system parameters, such as driving and interactions. It could be instructive to look for similar effects in other setups such as quantum metasurfaces [36]. There might also exist related nondecaying time-crystalline phases, mediated by the inherently long-ranged waveguide-mediated interactions [5,37,38].

Acknowledgments. I am grateful to A. V. Poshakinskiy for useful discussions. I also thank the Weizmann Institute of Science for temporarily hosting me at the last stages of this work. This work has been funded by the Russian Science Foundation Grant No. 20-12-00194.

[1] L. D'Alessio, Y. Kafri, A. Polkovnikov, and M. Rigol, From quantum chaos and eigenstate thermalization to statistical mechanics and thermodynamics, Adv. Phys. **65**, 239 (2016).

[2] N. Fayard, L. Henriet, A. Asenjo-Garcia, and D. E. Chang, Many-body localization in waveguide quantum electrodynamics, Phys. Rev. Res. **3**, 033233 (2021).

[3] F. Wilczek, Quantum Time Crystals, Phys. Rev. Lett. **109**, 160401 (2012).

[4] K. Sacha and J. Zakrzewski, Time crystals: a review, Rep. Prog. Phys. **81**, 016401 (2018).

[5] Z. Gong, R. Hamazaki, and M. Ueda, Discrete Time-Crystalline Order in Cavity and Circuit QED Systems, Phys. Rev. Lett. **120**, 040404 (2018).

[6] B. Buča, J. Tindall, and D. Jaksch, Non-stationary coherent quantum many-body dynamics through dissipation, Nat. Commun. **10**, 1730 (2019).

[7] D. Roy, C. M. Wilson, and O. Firstenberg, *Colloquium*: Strongly interacting photons in one-dimensional continuum, Rev. Mod. Phys. **89**, 021001 (2017).

[8] D. E. Chang, J. S. Douglas, A. González-Tudela, C.-L. Hung, and H. J. Kimble, *Colloquium*: Quantum matter built from nanoscopic lattices of atoms and photons, Rev. Mod. Phys. **90**, 031002 (2018).

[9] A. S. Sheremet, M. I. Petrov, I. V. Iorsh, A. V. Poshakinskiy, and A. N. Poddubny, Waveguide quantum electrodynamics: collective radiance and photon-photon correlations, arXiv:2103.06824.

[10] A. F. van Loo, A. Fedorov, K. Lalumiere, B. C. Sanders, A. Blais, and A. Wallraff, Photon-mediated interactions between distant artificial atoms, Science **342**, 1494 (2013).

[11] M. Mirhosseini, E. Kim, X. Zhang, A. Sipahigil, P. B. Dieterle, A. J. Keller, A. Asenjo-Garcia, D. E. Chang, and O. Painter, Cavity quantum electrodynamics with atom-like mirrors, Nature (London) **569**, 692 (2019).

[12] R. H. Dicke, Coherence in spontaneous radiation processes, Phys. Rev. **93**, 99 (1954).

[13] Y.-X. Zhang and K. Mølmer, Theory of Subradiant States of a One-Dimensional Two-Level Atom Chain, Phys. Rev. Lett. **122**, 203605 (2019).

[14] Y. Ke, A. V. Poshakinskiy, C. Lee, Y. S. Kivshar, and A. N. Poddubny, Inelastic Scattering of Photon Pairs in Qubit Arrays with Subradiant States, Phys. Rev. Lett. **123**, 253601 (2019).

[15] A. N. Poddubny, Quasiflat band enabling subradiant two-photon bound states, Phys. Rev. A **101**, 043845 (2020).

[16] R. Jones, G. Buonaiuto, B. Lang, I. Lesanovsky, and B. Olmos, Collectively Enhanced Chiral Photon Emission from an Atomic Array near a Nanofiber, Phys. Rev. Lett. **124**, 093601 (2020).

[17] Y.-X. Zhang and K. Mølmer, Subradiant Emission from Regular Atomic Arrays: Universal Scaling of Decay Rates from the Generalized Bloch Theorem, Phys. Rev. Lett. **125**, 253601 (2020).

[18] J. D. Brehm, A. N. Poddubny, A. Stehli, T. Wolz, H. Rotzinger, and A. V. Ustinov, Waveguide bandgap engineering with an array of superconducting qubits, npj Quantum Mater. **6**, 10 (2021).

[19] M. Zanner, T. Orell, C. M. F. Schneider, R. Albert, S. Oleschko, M. L. Juan, M. Silveri, and G. Kirchmair, Coherent control of a multi-qubit dark state in waveguide quantum electrodynamics, Nat. Phys. **18**, 538 (2022).

[20] A. V. Poshakinskiy and A. N. Poddubny, Dimerization of Many-Body Subradiant States in Waveguide Quantum Electrodynamics, Phys. Rev. Lett. **127**, 173601 (2021).

[21] O. Astafiev, Jr., A. M. Zagoskin, A. A. Abdumalikov, Y. A. Pashkin, T. Yamamoto, K. Inomata, Y. Nakamura, and J. S. Tsai, Resonance fluorescence of a single artificial atom, Science **327**, 840 (2010).

[22] E. L. Ivchenko, A. I. Nesvizhskii, and S. Jorda, Bragg reflection of light from quantum-well structures, Phys. Solid State **36**, 1156 (1994).

[23] A. N. Poddubny, M. M. Glazov, and N. S. Averkiev, Nonlinear emission spectra of quantum dots strongly coupled to a photonic mode, Phys. Rev. B **82**, 205330 (2010).

[24] F. Jahnke, C. Gies, M. Aßmann, M. Bayer, H. A. M. Leymann, A. Foerster, J. Wiersig, C. Schneider, M. Kamp, and S. Höfling, Giant photon bunching, superradiant pulse emission and excitation trapping in quantum-dot nanolasers, Nat. Commun. **7**, 11540 (2016).

[25] A. Shankar, J. T. Reilly, S. B. Jäger, and M. J. Holland, Subradiant-to-Subradiant Phase Transition in the Bad Cavity Laser, Phys. Rev. Lett. **127**, 073603 (2021).

[26] D. E. Chang, L. Jiang, A. V. Gorshkov, and H. J. Kimble, Cavity QED with atomic mirrors, New J. Phys. **14**, 063003 (2012).

[27] K. Lalumière, B. C. Sanders, A. F. van Loo, A. Fedorov, A. Wallraff, and A. Blais, Input-output theory for waveguide QED with an ensemble of inhomogeneous atoms, Phys. Rev. A **88**, 043806 (2013).

[28] See Supplemental Material at http://link.aps.org/supplemental/10.1103/PhysRevA.106.L031702 for theoretical details and results of auxiliary calculations, which includes Refs. [29–32].

[29] A. V. Poshakinskiy and A. N. Poddubny, Quantum Borrmann effect for dissipation-immune photon-photon correlations, Phys. Rev. A **103**, 043718 (2021).

[30] T. Orell, M. Zanner, M. L. Juan, A. Sharafiev, R. Albert, S. Oleschko, G. Kirchmair, and M. Silveri, Collective bosonic effects in an array of transmon devices, Phys. Rev. A **105**, 063701 (2022).

[31] K. Kaur, T. Sépulcre, N. Roch, I. Snyman, S. Florens, and S. Bera, Spin-Boson Quantum Phase Transition in Multilevel Superconducting Qubits, Phys. Rev. Lett. **127**, 237702 (2021).

[32] W. Nie, M. Antezza, Y.-x. Liu, and F. Nori, Dissipative Topological Phase Transition with Strong System-Environment Coupling, Phys. Rev. Lett. **127**, 250402 (2021).

[33] A. Albrecht, L. Henriet, A. Asenjo-Garcia, P. B. Dieterle, O. Painter, and D. E. Chang, Subradiant states of quantum bits coupled to a one-dimensional waveguide, New J. Phys. **21**, 025003 (2019).

[34] L. Landau and E. Lifshitz, *Quantum Mechanics* (Pergamon, New York, 1974).

[35] A. Blais, A. L. Grimsmo, S. M. Girvin, and A. Wallraff, Circuit quantum electrodynamics, Rev. Mod. Phys. **93**, 025005 (2021).

[36] J. Rui, D. Wei, A. Rubio-Abadal, S. Hollerith, J. Zeiher, D. M. Stamper-Kurn, C. Gross, and I. Bloch, A subradiant optical mirror formed by a single structured atomic layer, Nature (London) **583**, 369 (2020).

[37] V. K. Kozin and O. Kyriienko, Quantum Time Crystals from Hamiltonians with Long-Range Interactions, Phys. Rev. Lett. **123**, 210602 (2019).

[38] G. Buonaiuto, F. Carollo, B. Olmos, and I. Lesanovsky, Dynamical Phases and Quantum Correlations in an Emitter-Waveguide System with Feedback, Phys. Rev. Lett. **127**, 133601 (2021).